Morphological Phase Diagram for Lipid Membrane Domains with Entropic Tension

J. E. Rim,[1] T. S. Ursell,[2] R. Phillips,[2] and W. S. Klug[1]

[1]*Department of Mechanical and Aerospace Engineering, and California NanoSystems Institute, University of California, Los Angeles, California 90095, USA*

[2]*Department of Applied Physics, California Institute of Technology, Pasadena, California 91125, USA*

(Received 29 July 2010; published 3 February 2011)

Circular domains in phase-separated lipid vesicles with symmetric leaflet composition commonly exhibit three stable morphologies: flat, dimpled, and budded. However, stable dimples (i.e., partially budded domains) present a puzzle since simple elastic theories of domain shape predict that only flat and spherical budded domains are mechanically stable in the absence of spontaneous curvature. We argue that this inconsistency arises from the failure of the constant surface tension ensemble to properly account for the effect of entropic bending fluctuations. Formulating membrane elasticity within an entropic tension ensemble, wherein tension represents the free energy cost of extracting membrane area from thermal bending of the membrane, we calculate a morphological phase diagram that contains regions of mechanical stability for each of the flat, dimpled, and budded domain morphologies.

DOI: 10.1103/PhysRevLett.106.057801 PACS numbers: 87.16.D−, 62.10.+s

The importance of choosing an appropriate thermodynamic ensemble to account for different constraints imposed during a given experiment has been well recognized since the work of Gibbs [1]. Here we examine the effect of a loading ensemble on the stability of domain morphologies in phase-separated lipid membranes. In several ternary mixtures of lipids and cholesterol, two fluid phases coexist below a transition temperature [2], such that lipid domains form and can be observed with fluorescence microscopy [3–5]. These domains typically display one of three distinct morphologies with occasional transitions: flat, dimpled (partially budded), or fully budded. Equatorial views of phase-separated giant unilamellar vesicles (GUVs) are shown in Fig. 1 as examples of these morphologies, and the transitions between them, that are routinely observed [6].

A simple elastic model accounts for the transitions between flat and spherically budded domains [7,8]. The bending energy of the membrane competes with line tension at the domain phase boundary, tending to drive the domain toward curved shapes that decrease the boundary length while preserving domain area. This model predicts that above a critical size (or line tension) an initially flat domain deforms spontaneously into a completely spherical bud with an infinitesimal domain boundary, and that partially budded (dimpled) domains are mechanically stable only with nonzero spontaneous curvature. This latter prediction is inconsistent with experimental observations of dimpled domains in GUVs with no apparent spontaneous curvature [9,10]. Stable dimpled domains are crucial to the mechanical interactions between domains that arrest coalescence and spatially organize domains in a phase-separated membrane [9].

In the absence of spontaneous curvature, lateral membrane tension is a plausible candidate mechanism for stabilization of dimpled domains. This surface tension is often introduced as a Lagrange multiplier conserving the total area of the (nearly incompressible) membrane [e.g., [9,11,12]], and is determined by an interplay between membrane bending and conserved vesicle volume. Accordingly, observing that a nonspherical vesicle has an "excess" area greater than a spherical vesicle of the same volume, Yanagisawa, *et al.* [5] argued that domain budding could be halted once the domain deformations exhaust all excess area. For what appear optically to be spherical vesicles, this qualitative explanation does not identify the source of the extra area, nor how membrane area plays a role in the membrane energetics that govern morphology. Recent work by Semrau, *et al.* [12] showed that linear elastic stretching of the membrane provides a form of mathematical regularization that stabilizes dimpled domains. However, membrane stretching becomes significant only at tensions larger than $\sim 10^{-2} k_B T/\mathrm{nm}^2$ [13], which is roughly 2 orders of magnitude larger than tension estimates in experiments that observe dimpled domains [3,6,9,14], and hence membrane elastic stretch is an inappropriate physical mechanism. This lower tension regime is dominated by the entropy of microscopic undulations that store excess membrane area [13]; we refer to this as the entropic tension regime. In these settings, tension is commonly modeled as remaining constant as a membrane is deformed

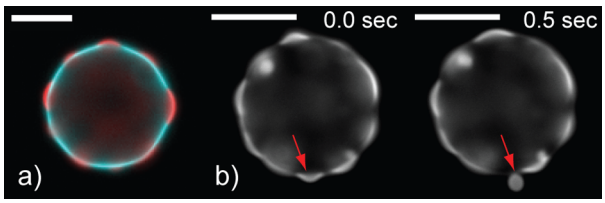

FIG. 1 (color online). Domain morphologies on vesicles [6]. (a) A phase-separated GUV showing dimpled domains (red) on the vesicle surface (blue). (b) A dimple-to-full bud transition indicated by the red arrows. Scale bars are 10 μm.

[2]. However, as we show in this work, constant tension is an inadequate assumption for explaining the stability of dimpled domains; rather it merely adjusts the relative stability of the flat and budded domain morphologies.

This array of clues suggests the need for a mathematical regularization other than constant tension to stabilize dimpled domains and allow for the accompanying transitions between morphologies. We resolve this puzzle with a careful treatment of the effects of thermal fluctuations on lateral tension. Specifically, in place of a membrane at constant tension, we consider the more realistic choice of a finite reservoir of thermal fluctuations. Incorporating the corresponding tension-area equation of state into the free energy of the simple elastic model, we calculate the phase diagram as a function of domain size and excess (thermal) membrane area, showing that the entropic tension ensemble renders all three domain morphologies stable in parameter ranges consistent with experiments.

Our model system is an initially flat circular domain embedded in a membrane matrix of a different phase, subject to a (for now, constant) far-field tension τ. We assume the domain is much smaller than the average radius of the vesicle, such that the ''background curvature'' of the vesicle is negligible, and thus we are essentially working with a flat membrane matrix. The boundary of the domain experiences a line tension γ due to the unfavorable interaction at the interface of the two phases. The free energy of the domain-matrix system as it deforms is the sum of the bending energy of the membrane, the interfacial energy from the line tension γ, and the work done by the membrane against tension [7,15], and is given by

$$G = \frac{\kappa}{2}\int_M (2H)^2 dA + 2\pi\gamma(r - r_0) + \tau\Delta A, \qquad (1)$$

where κ is the bending modulus, H is the mean curvature, M is the domain and matrix membrane, r is the interface radius of the deformed domain, and r_0 is the initial radius of the flat domain. ΔA is the additional area required to deform the domain and surrounding matrix membrane from an initially flat state. For simplicity, we assume κ is equal in the two phases, and we neglect the effects of Gaussian curvature, noting however that it becomes important when the Gaussian moduli of the two phases differ significantly relative to κ [14]. Eq. (1) can be written in closed analytic form by assuming that the domain deforms spherically while the matrix membrane remains flat [7], which, after normalizing the deformation energy by the bending energy of a sphere, $8\pi\kappa$, and the lengths by the so-called invagination length, $\xi = \kappa/\gamma$, takes the nondimensional form

$$\hat{G} \equiv \frac{G}{8\pi\kappa} = \left(1 + \frac{\sigma\rho_0^2}{8}\right)\left(1 - \frac{\rho^2}{\rho_0^2}\right) + \frac{1}{4}\left(\rho - \rho_0\right), \qquad (2)$$

where $\rho_0 = r_0/\xi$ and $\rho = r/\xi$ are the normalized initial and deformed interfacial radii, and $\sigma = \tau\xi^2/\kappa$ is the normalized membrane tension. The quadratic term represents the combined energy of bending and lateral tension, while the linear term represents the line energy of the domain boundary. This model predicts only flat ($\rho = \rho_0$) and spherical ($\rho = 0$) domains as stable morphologies. Larger values of the dimensionless domain size ρ_0 stabilize the spherical domain relative to the flat domain, whereas increasing the dimensionless membrane tension σ has the opposite effect.

To confirm that instability of partial buds ($0 < \rho/\rho_0 < 1$) is not simply an artifact of the assumptions on the deformed membrane geometry [16], we also performed numerical minimization of the nondimensionalized free energy of Eq. (1) by discretizing the domain and matrix with axisymmetric finite elements. Figure 2(a) shows the numerical minimum free energy as a function of deformed domain radius for systems with select values of domain size ρ_0 and membrane tension σ. Figure 2(b) shows meridional curves of the finite element model obtained by quasi-Newton numerical minimization of the free energy at several prescribed values of the deformed domain radius with $\sigma = 0.25$. For typical lipid membranes with $\kappa = 25k_BT$ [17] and $\xi = 50$ nm [18], the values of ρ_0 and σ used in the calculations correspond to domain sizes $25\ \text{nm} \le r_0 \le 500\ \text{nm}$ and membrane tensions $2.5 \times 10^{-6}k_BT/\text{nm}^2 \le \tau \le 10^{-2}k_BT/\text{nm}^2$, as compared to experimental values of $\sim 10^{-5}k_BT/\text{nm}^2$ [3]. For comparison, the results of the simplified analytical model, Eq. (2), are plotted as dashed lines, demonstrating that the errors of the simplified analytical model are small, and more importantly, that the instability of the partially budded domains is not an artifact of the geometric assumptions. The failure of the constant tension ensemble to predict stable dimpled domains foreshadows the need to consider mechanisms that alter lateral tension as a function of membrane deformation.

At finite temperature, a finite amount of excess area is stored in the thermal undulations of the membrane. For a membrane with actual area A, the thermal undulations are superimposed on the projected, or measurable area, A_p, such that $A_p < A$. This excess area $A - A_p$, can be accessed by the deforming membrane at exponentially increasing membrane tension, as demonstrated experimentally [17].

To model the coupling between entropic tension and membrane deformation, imagine a ''thermal reservoir'' at temperature $T > 0$ with actual area A and projected area A_p, coupled to an initially flat domain and matrix membrane whose projected and actual areas are equal to A_p, as shown in Fig. 3. The coupling allows the flow of lipids from one region to the other, where the total amount of lipids in the ensemble is conserved, which results in equal tension in both regions. As the zero-temperature domain-matrix system deforms at constant projected area, it pulls in an area ΔA from the thermal reservoir. The projected area of the thermal reservoir, A_p, remains unchanged, but its actual area decreases from A to $A - \Delta A$. A straightforward

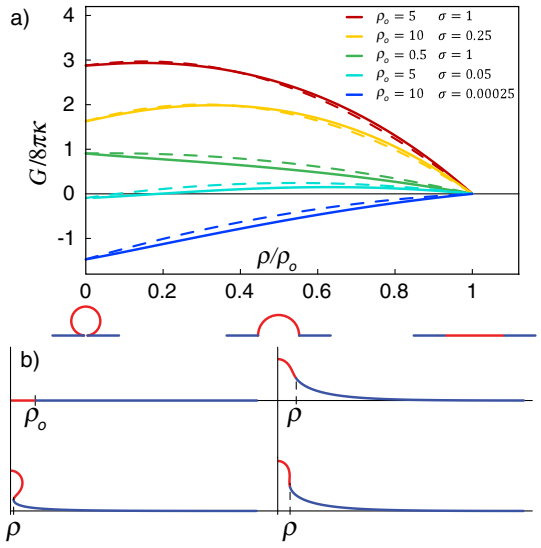

FIG. 2 (color online). Energies and shapes of deformation. (a) Normalized free energy of a budding membrane as a function of domain radius, ρ, relative to the flat radius, ρ_0, in the constant tension ensemble, for a few values of domain size ρ_0 and normalized surface tension σ. The solid lines are the numerical results; the dashed lines correspond to the simplified analytical model. (b) Meridional curves from axisymmetric finite element numerical minimization of free energy for $\sigma = 0.25$ for $\rho/\rho_0 = \{1, \frac{3}{4}, \frac{1}{2}, \frac{1}{8}\}$, clockwise from upper left. In dimensionless form, these configurations depend only on σ, and not on ρ_0. Note that while the length of the meridional curve changes with the deformation, the area of the domain is preserved.

calculation gives the entropic equation of state for the surface tension [19], with the robust approximation

$$\tau \simeq \frac{\pi^2\kappa}{a_o} e^{-(8\pi\kappa/k_BT)(A-A_p-\Delta A/A_p)}, \tag{3}$$

where $a_0 \approx 0.7$ nm^2 is the area per lipid molecule for a typical bilayer [20]. Integration of Eq. (3) gives the free energy

$$G_{\text{ent}} = \int_0^{\Delta A} \tau d[\Delta A'] = \frac{A_p \pi k_B T}{8a_o} e^{-(8\pi\kappa/k_BT)(A-A_p/A_p)} \times (e^{(8\pi\kappa/k_BT)(\Delta A/A_p)} - 1), \tag{4}$$

which simplifies to a constant tension ensemble for $\Delta A/A_p \ll k_BT/8\pi\kappa$.

The contributions from membrane bending and phase boundary line tension remain unchanged from Eq. (2), and the normalized total free energy of membrane deformation in the entropic tension ensemble is

$$\hat{G} = \left(1 - \frac{\rho^2}{\rho_0^2}\right) + \frac{1}{4}(\rho - \rho_0) + \frac{Nk_BT}{64\kappa} e^{-(8\pi\kappa\varepsilon/k_BT)} \left[e^{(8\pi\kappa\alpha/k_BT)(1-(\rho^2/\rho_0^2))} - 1 \right], \tag{5}$$

where $N = A_p/a_o$ is the size of the thermal reservoir ($\sim$ number of lipids in the reservoir), $\varepsilon = (A - A_p)/A_p$ is the excess area fraction stored in the membrane undulations, and $\alpha = \pi r_0^2/A_p = A_o/A_p$ is the domain area fraction.

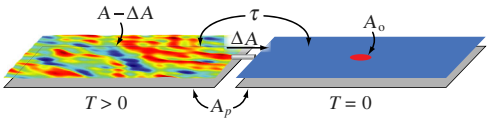

FIG. 3 (color online). Schematic of the entropic tension ensemble. The thermal reservoir (left) at a finite temperature T initially has an actual area A and projected area A_p. The domain-matrix system (right) is at $T = 0$, with actual and projected areas equal to A_p. The domain has an area A_o, and ΔA is the area required from the reservoir to deform the domain-matrix system from the flat state. The small pipe represents a perfect thermal insulator that permits the flow of lipids from one region to the other, where the total amount of lipids in the ensemble is conserved, resulting in equal tension in both regions.

The free energy of Eq. (5) is then a function of the size of the reservoir N, the domain area fraction α, and the excess area fraction ε. At zero tension, the reservoir achieves a maximum excess area fraction $\varepsilon \propto \ln(N)$. The reservoir supplies the higher-order dependence on ρ in the free energy necessary to stabilize dimples, and thus the set of equilibrium shapes includes combinations of flat, dimpled, and budded domains depending on location within the 3D (N, α, ε) phase space. Figure 4 shows two 2D slices through the 3D phase diagram for $N = 4.5 \times 10^8$ and $N = 7 \times 10^7$, corresponding to membrane areas of $A_p = \pi(10\ \mu\text{m})^2$ and $A_p = \pi(4\ \mu\text{m})^2$, respectively. These 2D phase diagrams show regions where flat, dimpled, and fully budded morphologies are each stable. In addition, regions of metastability appear where transitions between two or even three (for $N = 7 \times 10^7$) morphologies may occur.

Figure 4(a) shows a slice through this three parameter (N, α, ε) phase diagram containing one and two phase regions, while Fig. 4(b) contains all phases, except flat-dimple coexistence. To illustrate the energy landscape in the tristable region of Fig. 4(b), we plot the normalized free energy along with the individual contributions from bending, line tension, and entropic surface tension in Fig. 4(c). In this region the dimpled state is the global energy minimum, while the flat and budded morphologies are local minima. Figure 4(c) shows how the Gaussian form of $\hat{G}_{\text{ent}}(\rho)$ offsets the negative curvature of $\hat{G}_{\text{bend}}(\rho)$ to yield a local energy minimum at an intermediate value of ρ/ρ_0 in $\hat{G}(\rho)$. For this case, the dimpled state is separated from the flat and fully budded states by barriers of $\approx 6.6k_BT$ and $640k_BT$, respectively.

The range of $0.01 < \varepsilon < 0.03$ in Fig. 4(b) translates to a range of lateral tensions $0.66k_BT/\text{nm}^2 > \tau > 2 \times 10^{-6}k_BT/\text{nm}^2$, with experimental values on the order of $\sim 10^{-5}k_BT/\text{nm}^2$ [3]. The existence of stable regions for each of the morphologies over this range is consistent with the fact that all three morphologies are observed in experimental systems. Both α and ε are experimental control

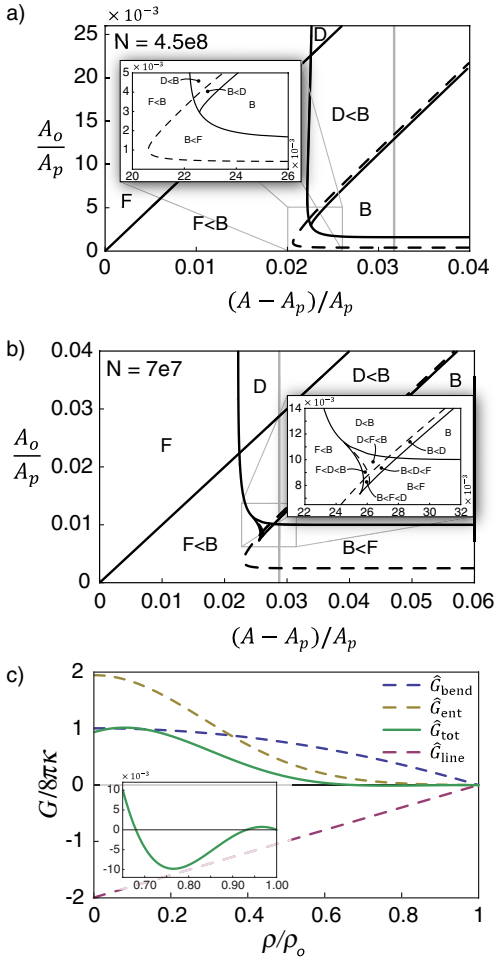

FIG. 4 (color online). Morphological phase diagrams for (a) $N = 4.5 \times 10^8$ and (b) $N = 7 \times 10^7$, with bending modulus $\kappa = 25 k_B T$. "F", "D", and "B" represent the flat, dimpled, and fully budded domains. Regions with more than one letter indicate metastability, with letters ordered in increasing free energy. Solid lines are "hard" phase boundaries, across which morphologies appear or disappear. Dashed lines are "preference" boundaries, indicating changes in the energetic ranking of metastable morphologies. The vertical grey lines are the excess area fraction in the reservoir at zero tension. (c) The normalized free energy, $G/8\pi\kappa$, as a function of ρ/ρ_0 for $N = 7 \times 10^7$, $A_o/A_p = 0.01$, and $(A - A_p)/A_p = 0.026$. The lowest-energy state (inset) at $\rho/\rho_0 \simeq 0.76$ is a dimple, while flat and full buds are metastable.

parameters. For instance, ε can be adjusted either by micropipette aspiration [13] or by controlled thermal expansion of the membrane. On the other hand, increases in α occur passively as pairs of domains spontaneously coalesce into a single larger domain. As complete phase separation into two simply connected domains is the thermodynamic ground state, an "upward" flow through the phase diagrams in Fig. 4 is generally expected in experiment, although trajectories are not entirely vertical due to conserved vesicle volume. For example, consider the trajectory of an initially small, flat domain coalescing with a flat domain, crossing the horizontal preference line in the phase diagram to yield a budded domain, which might coalesce with another causing traversal into the dimpled region of the phase diagram. Indeed, such sequences of coalescence that link to domain morphology have been observed experimentally [6].

This static model of domain mechanical stability, and corresponding morphological phase diagrams, is an initial step toward understanding domain dynamics in vesicles *in vitro* and cell membranes *in vivo*. A more complete picture requires accounting for the effects of the coupled lipid and solvent hydrodynamics, the chemical kinetics of phase coalescence, and the potential roles of proteins in lipid organization.

We thank C. Haselwandter for helpful comments. W. S. K. and J. E. R. were supported by NSF CAREER Award CMMI-0748034. R. P. and T. S. U. were supported by a Collaborative Innovation Award of the Howard Hughes Medical Institute, and the National Institutes of Health through NIH Award number R01 GM084211 and the Director's Pioneer Award.

[1] J. W. Gibbs, *On the Equilibrium of Heterogeneous Substances*, The Collected Works of J. Williard Gibbs Vol. 1 (Yale University Press, New Haven, 1957). .
[2] R. Lipowsky and R. Dimova, J. Phys. Condens. Matter **15**, S31 (2003).
[3] T. Baumgart, S. T. Hess, and W. W. Webb, Nature (London) **425**, 821 (2003).
[4] S. L. Veatch and S. L. Keller, Phys. Rev. Lett. **89**, 268101 (2002).
[5] M. Yanagisawa *et al.*, Biophys. J. **92**, 115 (2007).
[6] T. S. Ursell, *Bilayer Elasticity in Protein and Lipid Organization* (VDM Verlag, Berlin, 2009).
[7] R. Lipowsky, J. Phys. II (France) **2**, 1825 (1992); R. Lipowsky, Biophys. J. **64**, 1133 (1993).
[8] F. Jülicher and R. Lipowsky, Phys. Rev. Lett. **70**, 2964 (1993).
[9] T. Ursell, W. Klug, and R. Phillips, Proc. Natl. Acad. Sci. U.S.A. **106**, 13301 (2009).
[10] Spontaneous curvature is a preferred mean curvature that reflects an asymmetry in the lipid bilayer.
[11] F. Jülicher and R. Lipowsky, Phys. Rev. E **53**, 2670 (1996).
[12] S. Semrau *et al.*, Biophys. J. **96**, 4906 (2009).
[13] E. Evans and W. Rawicz, Phys. Rev. Lett. **64**, 2094 (1990).
[14] T. Baumgart *et al.*, Biophys. J. **89**, 1067 (2005).
[15] P. Sens and M. S. Turner, Phys. Rev. E **73**, 031918 (2006).
[16] In reality, the slope is continuous across the phase boundary (e.g., [3]).
[17] W. Rawicz *et al.*, Biophys. J. **79**, 328 (2000).
[18] A. Tian *et al.*, Phys. Rev. Lett. **98**, 208102 (2007).
[19] W. Helfrich and R. M. Servuss, Nuovo Cimento **3**, 137 (1984).
[20] H. I. Petrache, S. W. Dodd, and M. F. Brown, Biophys. J. **79**, 3172 (2000).